Energy xxx (2013) 1–10

Contents lists available at SciVerse ScienceDirect

Energy

journal homepage: www.elsevier.com/locate/energy

Experimental investigation of partial shading scenarios on PV (photovoltaic) modules

Alberto Dolara [a], George Cristian Lazaroiu [b,*], Sonia Leva [a], Giampaolo Manzolini [a]

[a] Department of Energy, Politecnico di Milano, Via Lambruschini 4, 20156 Milan, Italy
[b] Department of Power Systems, University POLITEHNICA of Bucharest, Splaiul Independentei 313, 060042 Bucharest, Romania

ARTICLE INFO

Article history:
Received 16 October 2012
Received in revised form
9 February 2013
Accepted 9 April 2013
Available online xxx

Keywords:
Energy
Sustainability
Photovoltaic modules
Partial shading
Power losses

ABSTRACT

The power generation of photovoltaic systems is significantly affected by partial or complete shading of its cells and it depends of the PV array configuration, shading characteristics, and presence of bypass diode. The paper deals with the investigation of the impact of partial shading on poly-crystalline and mono-crystalline PV modules operation. Several experiments consisting of measuring the current–voltage and power–voltage curves of photovoltaic modules of a real PV plant, both unshaded and applying shading profiles, have been carried out in clear sunny days. The experimental analysis can be applied to derive mathematical models for evaluating the power losses under shading conditions influencing PV modules operation.

1. Introduction

The European Union has set targets to achieve clean and secure energy for tomorrow. The energy efficiency and renewable energy policies are adopted with the goal to reach the EU 2020 targets (20% reduction in greenhouse gas emissions, 20% improvement in energy efficiency and 20% of renewable in EU energy consumption). The renewable sources can be used in small and decentralized power plants or in large generation systems [1–3]. They are modular and can be built in small size modules to be used in different locations. The natural variability of environmental conditions and nonlinear behavior of photovoltaic generators make the utilization of photovoltaic energy a challenging task. The photovoltaic (PV) modules are composed of a number of cells connected in series, assumed to be identical with respect to electrical properties. Still, these cells behaves differently when are operating in non-ideal conditions determining mismatch losses of PV system. The design process of PV systems – regarding both energy production and efficiency – requires the evaluation of their operation in non-ideal conditions [4–8]. Thus, the reduced irradiation determined by shadows projected on PV modules causes a power–voltage characteristic curve deviating from standard form, function of shadow's geometric characteristics (like distance, shape, size, intensity) and electrical characteristics of the photovoltaic cells [9–11].

The influence of shading objects on PVs energy production, function of their relative position, represents a difficult task. The shaded cells absorb electric power generated by the unshaded cells, causing hot spots that can irreversible damage the module. The influence of shading conditions on the mismatch of PV systems is investigated in Refs. [12–15]. The bypass-diodes influence on mismatched PV systems is investigated in Refs. [16–18], illustrating the I–V characteristics of the whole PV module and the PV module output power. The Newton–Raphson method, used for iterative solving the PV nonlinear equations, is applied for investigating the mismatched PV systems in Refs. [19–22]. Software implemented simulation models for analysis of shadowing effects on PV systems are proposed by using PV-specific programs in Refs. [23,24], MATLAB in Ref. [25], PSpice in Refs. [26,27], PSIM in Ref. [28], and EMTP in Ref. [29]. Modeling guidelines and a benchmark system – in the PSCAD/EMTDC software environment – for power system simulation studies of grid-connected, three-phase, single-stage Photovoltaic (PV) systems that employ a voltage-sourced converter (VSC) as the power converter are proposed in Ref. [30].

* Corresponding author. Tel: +40 724528546; fax: +40 214029440.
E-mail addresses: alberto.dolara@mail.polimi.it (A. Dolara), clazaroiu@yahoo.com (G.C. Lazaroiu), sonia.leva@polimi.it (S. Leva), giampaolo.manzolini@polimi.it (G. Manzolini).

0360-5442/$ – see front matter © 2013 Elsevier Ltd. All rights reserved.
http://dx.doi.org/10.1016/j.energy.2013.04.009

The maximum power reduction due to the inefficiency of maximum power point tracking algorithms affected by partial shading conditions is investigated in Refs. [31,32], while modified PV arrays for improvement of system performance under nonuniform irradiation conditions are proposed in Refs. [33–35]. However, significant modeling complexity and high computational times for accurate calculation of current–voltage and power–voltage curves are required.

In the present paper, an experimental study of the PV energy production losses under partial shading conditions is conducted on a real PV plant within the Solar Tech Lab of Politecnico di Milano, Italy. The PV plant is composed of mono-crystalline and poly-crystalline modules, each module with 60 series-connected cells and three bypass diodes. Each module consists of 6 columns, each with 10 cells, geometrically placed on its long side. The bypass diodes are connected every two columns, dividing the module in three equal subsections. Different shading scenarios are analyzed, considering a single-cell and a PV module shaded from 0% to 100%. The current–voltage and power–voltage characteristic curves measured in outdoor conditions are reported. The performed experimental tests provide an investigation of shadow effects on the main electrical behavior of the PV modules and can be used in deriving mathematical models for evaluating the power losses under nonuniform irradiation conditions.

2. Experimental setup and procedure of experiment

2.1. Description of Solar Tech Lab and experimental setup

The layout of Solar Tech Lab are illustrated in Fig. 1, [36]. The system is composed of 21 modules: 19 modules (10 poly-crystalline and 9 mono-crystalline) are placed on support structures with a fixed tilt angle of 30° and the last 2 modules (1 poly-crystalline and 1 mono-crystalline) are placed on a structure that allows manual adjustment of the tilt angle; all modules are facing South. Each module is connected to the low voltage distribution grid through micro-inverters that optimize the operating conditions.

The geographical coordinates of the Solar Tech Lab are latitude 45.502941° N and longitude 9.156577° E. An European solar radiation database, using a solar radiation model and climatic data integrated within the Photovoltaic Geographic Information System (PVGIS), is presented in Ref. [37].

Table 1
Meteorological station main characteristics.

	Net radiometer (LSI DPD504)[42]	Pyranometer (LSI, DPA253) [43]
Measurements range [W/m^2]	<2000	<2000
Spectral range	0.3–60 μm	305–2800 nm
Total achievable daily uncertainity	<5%	<5%
Non-linearity	<1.5%	<4%
Thermal drift	<2%	<1.2%

The conducted experiments campaign recorded the current–voltage and calculated the power–voltage characteristics of the various modules, in different operating conditions. The requirements for the measurements of photovoltaic current–voltage characteristics are established in standard IEC 60904-1 [38]. The procedures for temperature and irradiance corrections to measured *I–V* characteristics of photovoltaic devices are specified in standard IEC 60891 [39]. The minimum requirements for system documentation, commissioning tests and inspection of grid connected PV systems are stipulated in IEC 62446 [40]. Examples of measurements carried out accordingly to the previously mentioned standards are reported in Ref. [41]. In the present paper, the absolute performances of the modules were not investigated. Instead, the comparison of the performances of the modules under different shading conditions was investigated.

The environmental conditions were monitored with a meteorological station equipped with solar radiation, temperature-humidity and wind speed/direction sensors. The possibility to measure ambient temperature and wind conditions is not necessary for the performed analysis within this work. These measurements are important for the development of PV predictive models. Solar irradiation is measured with three different sensors: a net radiometer for the measurement of the Direct Normal Irradiance (DNI) and two pyranometers for the measurement of total, respectively diffuse, irradiation on a horizontal plane. The main characteristics of solar radiation measuring equipments are reported in Table 1.

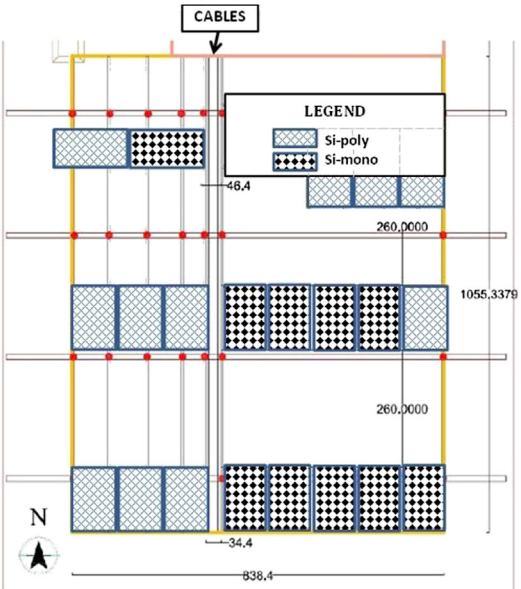

Fig. 1. PV modules installed at Solar Tech Lab, Politecnico di Milano.

Please cite this article in press as: Dolara A, et al., Experimental investigation of partial shading scenarios on PV (photovoltaic) modules, Energy (2013), http://dx.doi.org/10.1016/j.energy.2013.04.009

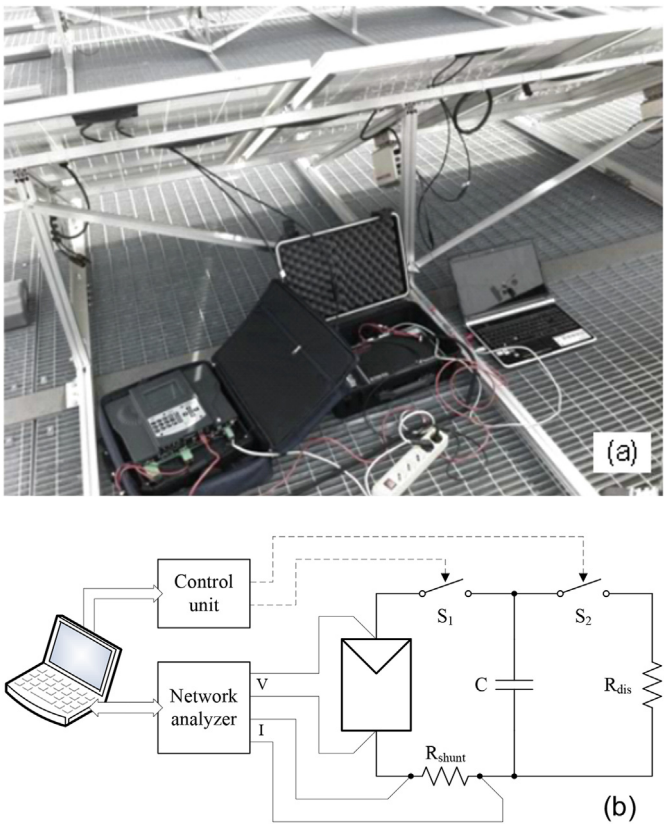

Fig. 2. Measurement equipments recording the PV characteristics: (a) field-test measurements; (b) operating principle.

The electrical measurements were performed using prototype and market-available measuring equipments shown in Fig. 2(a). The operating principle of the measurement instrument is illustrated through the block diagram shown in Fig. 2(b). The switching device S_1 operates the connection of PV module with the load. The switching device S_2 is used to discharge and to hold uncharged the capacitor. The switching devices are automatically managed by the control unit. The test starts by opening S_2 and closing S_1.

The current produced by the PV module gradually charge the capacitor. The test terminates when the capacitor voltage reaches the value of the open circuit voltage of the PV module. The capacitance is sized to ensure that the test duration is about 0.2 s when the irradiation is 1000 W/m^2. At the end of the test, S_1 opens and S_2 closes, allowing the discharge of the capacitor on the dissipation resistor R_{dis}. A network analyzer in "transient analysis" mode carries out and stores the values of voltage and current. The analyzer is equipped with 12-bit A/D converters that simultaneously sample the voltage and current signals. The sampling frequency is 12.5 kHz. The voltage measurement is carried out by using direct connection, while current measurement is indirect, through the shunt resistor R_{shunt}. The accuracy of the network analyzer input channels is reported in Table 2. The PC, interfaced with the instrument management software, coordinates and controls the measuring systems. The acquired data are stored at the end of each test. The instrument is programmed to perform a test in 0.5 s. The data were recorded with transducers within ±1% accuracy. The current–voltage characteristic is composed of 6250 pairs of values.

2.2. Experimental procedure

The current–voltage characteristic of a PV module requires the measurement of voltage and current values at its terminals. As this characteristic of a PV module varies with the irradiation, as well as with cell temperature, during the current–voltage characteristic measurement is necessary that these parameters remain as constant as possible. For the field measurements, the irradiation may vary quickly due to rapid changes in the atmospheric conditions, while the thermal dynamics are much slower. The field-test conditions require to carry out the current–voltage characterization test in the shortest possible time. Hence, the PV module is connected to the automatic instrument previously described, which must be able to vary the load connected to the PV module, as well as to measure and store the current and voltage values. The solar radiation, ambient temperature and wind speed were monitored by the meteorological station. The cell and module temperatures were monitored by using a thermal camera and a thermocouple placed on the back of the module.

The purpose of the conducted investigations is to record and compare the current–voltage and power–voltage characteristics obtained under different shading conditions. The measured data are processed to be compared, but they are not reported at standard test conditions (STC).

Experiments are performed on PV modules under various shading conditions. The shading process eliminates both the direct solar and diffuse radiation incident on the module. The following shading cases were considered:

- single-cell shaded with vertical, as well as horizontal, shading profiles;
- module shaded with vertical, horizontal, and diagonal shading profiles.

The measurements campaign is conducted on poly-crystalline and mono-crystalline modules.

2.2.1. Experimental procedure for shading a PV single-cell

For the poly-crystalline, as well as for the mono-crystalline PV modules, experiments are performed applying two shading scenarios to a single-cell:

- shading profile from right-to-left, increasing the shaded area from 0% to 100%, as illustrated in Fig. 3(a);
- shading profile from bottom-to-top, increasing the shaded area from 0% to 100%, as illustrated in Fig. 3(b).

For each type of PV module and shading scenario, the current–voltage and power–voltage curves are recorded. The performed tests have the purpose to analyze the influence that a shading process applied to a single-cell is inducing on the entire PV module.

Table 2
Characteristic data of the measurement equipment.

	Full scale (FS)	Accuracy: 1–10% of FS	Accuracy: 10–130% of FS	Accuracy: 130–150% of FS
Voltage input	100 V	1 V	100 mV	1 V
Current input from transducer	3 V	30 mV	3 mV	30 mV

Please cite this article in press as: Dolara A, et al., Experimental investigation of partial shading scenarios on PV (photovoltaic) modules, Energy (2013), http://dx.doi.org/10.1016/j.energy.2013.04.009

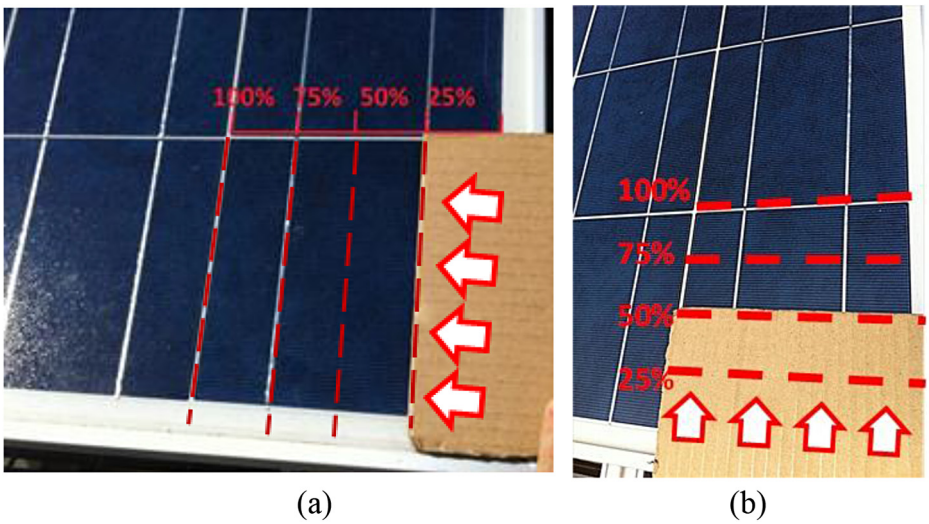

Fig. 3. Shading profile of a single-cell: (a) Right-to-left, (b) Bottom-to-top.

2.2.2. Experimental procedure for shading a PV module

For the poly-crystalline, as well as for the mono-crystalline PV modules, new experiments are performed applying three shading scenarios to the PV module:

- vertical shading profile, increasing the shaded area from 0% to 100%, as illustrated in Fig. 4(a);
- horizontal shading profile, increasing the shaded area from 0% to 100%, as illustrated in Fig. 4(b);
- diagonal shading profile, increasing the shaded area from step 0 to step 5, as illustrated in Fig. 4(c);

For each type of PV module and shading scenario, the current–voltage and power–voltage curves are recorded.

2.2.3. Measurements and data processing

Measurements are taken recording the environmental conditions as well as the electrical and thermal variables related to the module. All tests on poly-crystalline modules were carried out in the middle of the day of a clear and sunny day, as well as the tests on mono-crystalline modules (one day for tests on poly-crystalline modules, and another day for tests on mono-crystalline ones). The duration of a single test is less than a minute, considering both the time to the measurement of current–voltage and power–voltage curves, and the time for the positioning of the obstacle that creates the shading.

Accordingly to [38] each current–voltage curve was measured in natural sunlight only when global solar irradiance is not fluctuating more than 1% during a measurement and the irradiance is at least 800 W/m^2 (exceeding 850 W/m^2). During all tests, no significant cell and module temperature variations were registered, while the irradiation was between 850 W/m^2 and 950 W/m^2. In order to compare the measured data, they were corrected considering the reference irradiance of 1000 W/m^2; since the temperature was constant, no temperature correction was introduced. In Ref. [39], three correction procedures are proposed; in this work correction procedure 2 (based on a one-diode model of PV devices) is taken into account. The correction procedure is defined by:

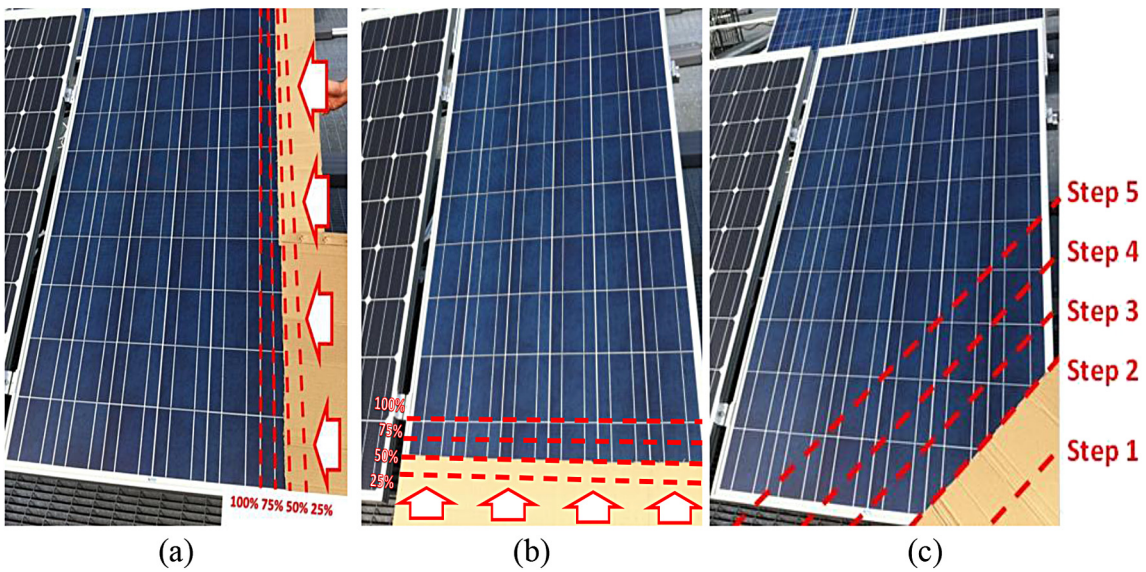

Fig. 4. Shading scenarios of the PV module: (a) Vertical shading profile, (b) Horizontal shading profile, and (c) Diagonal shading profile.

Please cite this article in press as: Dolara A, et al., Experimental investigation of partial shading scenarios on PV (photovoltaic) modules, Energy (2013), http://dx.doi.org/10.1016/j.energy.2013.04.009

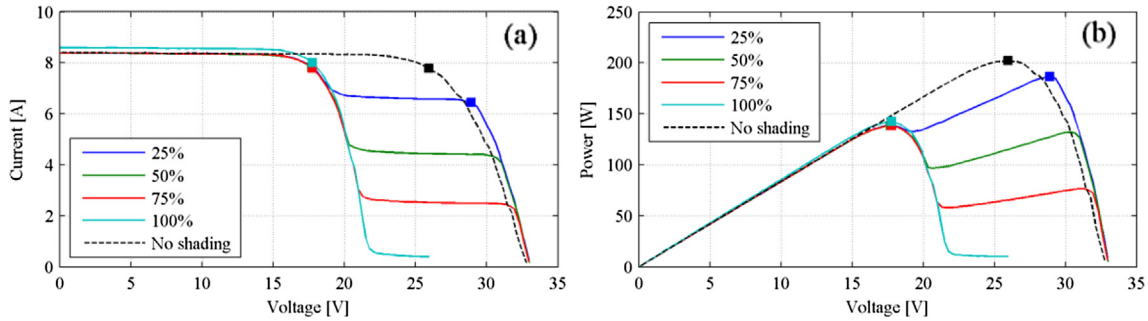

Fig. 5. Recorded characteristics of poly-crystalline modules, referred to 1000 W/m^2: (a) current–voltage, and (b) power–voltage. Single-cell shading profile from right to left.

$$I_{\text{ref}} = I_m \cdot (1 + \alpha_{\text{rel}} \cdot (T_2 - T_1)) \cdot \frac{G_{\text{ref}}}{G_m} \tag{1}$$

$$V_{\text{ref}} = V_m + V_{\text{OC}m} \cdot \left(\beta_{\text{rel}} \cdot \left(T_{\text{ref}} - T_m \right) + a \cdot \ln\left(\frac{G_{\text{ref}}}{G_m} \right) \right) - R_S' \cdot \left(I_{\text{ref}} - I_m \right) - k' I_{\text{ref}} \left(T_{\text{ref}} - T_m \right) \tag{2}$$

where the subscripts ref and m refer to the reference, respectively the measured, conditions; V is the voltage; V_{OC} is the module open voltage; I is the current; G is the irradiance; α_{rel} and β_{rel} are the relative current and voltage temperature coefficients; a is a constant (usually taken equal to 0.06); R_S' is the internal series resistance; k' can be interpreted as the temperature coefficient of the internal series resistance. Considering the values of irradiance during test, it is possible to strongly simplify the correction relations as:

$$I_{\text{ref}} = I_m \cdot \frac{G_{\text{ref}}}{G_m} \tag{3}$$

$$V_{\text{ref}} \cong V_m \tag{4}$$

Therefore, the MPP at reference solar irradiation of 1000 W/m^2 is:

$$P_{\text{MPP ref}} = P_{\text{MPP }m} \cdot \frac{G_{\text{ref}}}{G_m} \tag{5}$$

The power $P_{\text{MPP ref}}$ in (5) does not represent the maximum power at STC conditions, but it is only a value for comparing the performances of the module under different shading conditions and considering the same irradiance and the same temperature.

3. Results and discussion

3.1. Experimental results in case of PV single-cell shading

The results obtained from experimental tests performed on modules, with shading scenarios applied to a single-cell (see Section 2.2.1), are illustrated in Figs. 5–8.

The obtained current–voltage and power–voltage characteristics for the poly-crystalline PV module are illustrated in Figs. 5 and 6, for the two experimentally tested shading scenarios of a single-cell, reported to the 1000 W/m^2 solar irradiation. Figs. 7 and 8 illustrate the current–voltage and the power–voltage characteristics obtained for the mono-crystalline PV module, for the two experimentally tested shading scenarios of a single-cell, reported to the 1000 W/m^2 solar irradiation.

Fig. 5, respectively Fig. 7, illustrates the current–voltage and power–voltage curves of a poly-crystalline, respectively mono-crystalline, PV module with a single-cell shaded from 0% (unshaded conditions) to 100%, from right-to-left. The points (V_{MPP}, I_{MPP}) and (V_{MPP}, P_{MPP}), for each shading condition, are illustrated.

Fig. 6, respectively Fig. 8, illustrates the current–voltage and power–voltage curves of a poly-crystalline, respectively mono-crystalline, PV module with a single-cell shaded from 0% to 100%, from bottom-to-top. The points (V_{MPP}, I_{MPP}) and (V_{MPP}, P_{MPP}), for each shading condition, are highlighted.

3.2. Experimental results in case of PV module shading

Figs. 9–11 illustrate the current–voltage and the power–voltage characteristics obtained for the poly-crystalline PV modules, for the three experimentally tested shading scenarios described in Section 2.2.2. Figs. 12–14 illustrate the current–voltage and the power–voltage characteristics obtained for the mono-crystalline PV modules, for the same experimentally tested shading scenarios.

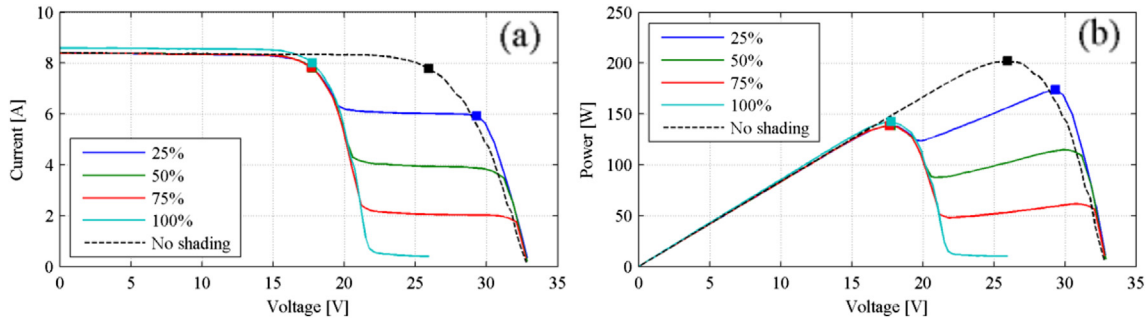

Fig. 6. Recorded characteristics of poly-crystalline modules, referred to 1000 W/m^2: (a) current–voltage, and (b) power–voltage. Single-cell shading profile from bottom-to-top.

Please cite this article in press as: Dolara A, et al., Experimental investigation of partial shading scenarios on PV (photovoltaic) modules, Energy (2013), http://dx.doi.org/10.1016/j.energy.2013.04.009

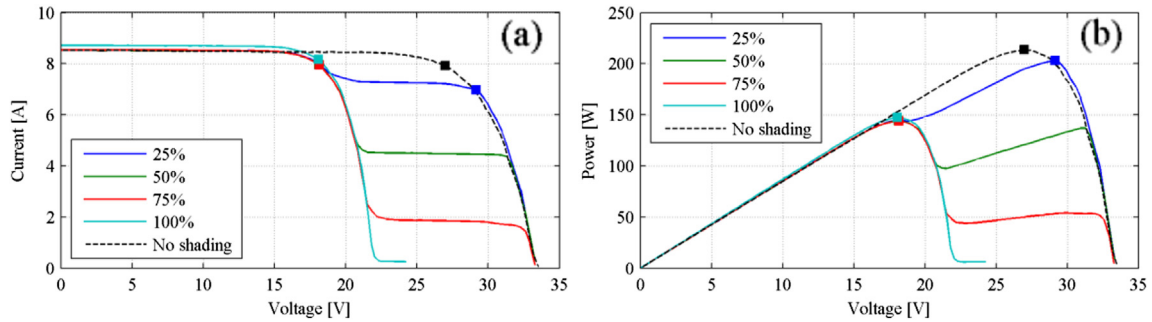

Fig. 7. Recorded characteristics of mono-crystalline modules, referred to 1000 W/m^2: (a) current–voltage, and (b) power–voltage. Single-cell shading profile from right-to-left.

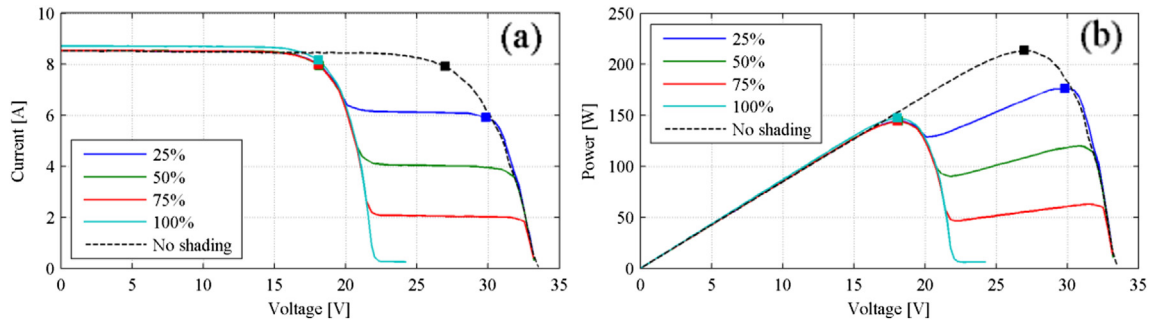

Fig. 8. Recorded characteristics of mono-crystalline modules, referred to 1000 W/m^2: (a) current–voltage, and (b) power–voltage. Single-cell shading profile from bottom-to-top.

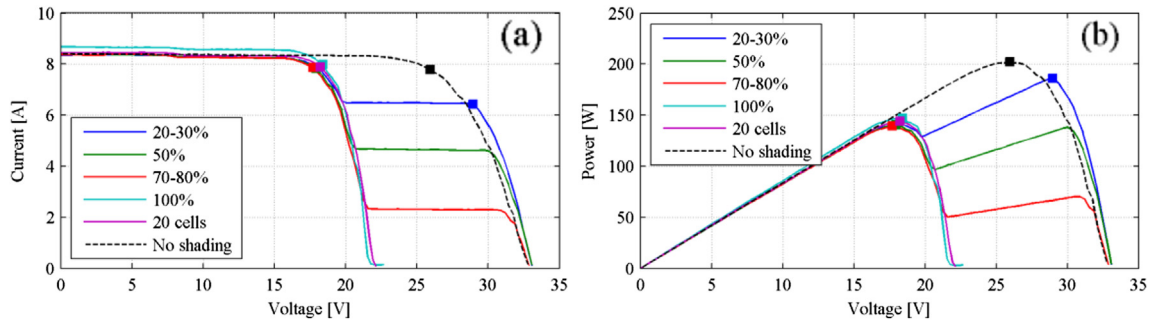

Fig. 9. Recorded characteristics of poly-crystalline modules, referred to 1000 W/m^2: (a) current–voltage, and (b) power–voltage. Vertically shading profile.

Fig. 9, respectively Fig. 12, illustrates the current–voltage and power–voltage curves of a poly-crystalline, respectively mono-crystalline, PV module with 10 cells vertically shaded from 0% to 100%, and with 20 cells vertically shaded. The points (V_{MPP}, I_{MPP}) and (V_{MPP}, P_{MPP}), for each shading condition, are illustrated.

Fig. 10, respectively Fig. 13, illustrates the current–voltage and power–voltage curves of a poly-crystalline, respectively mono-crystalline, PV module horizontally shaded for the most significant cases, i.e. 0%, 50%, and 100%. The points (V_{MPP}, I_{MPP}) and (V_{MPP}, P_{MPP}), for each shading condition, are highlighted.

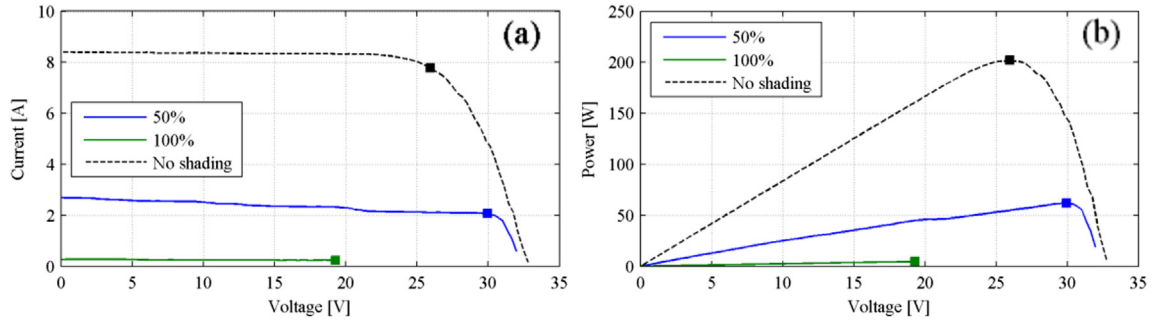

Fig. 10. Recorded characteristics of poly-crystalline modules, referred to 1000 W/m^2: (a) current–voltage, and (b) power–voltage. Horizontally shading process.

Please cite this article in press as: Dolara A, et al., Experimental investigation of partial shading scenarios on PV (photovoltaic) modules, Energy (2013), http://dx.doi.org/10.1016/j.energy.2013.04.009

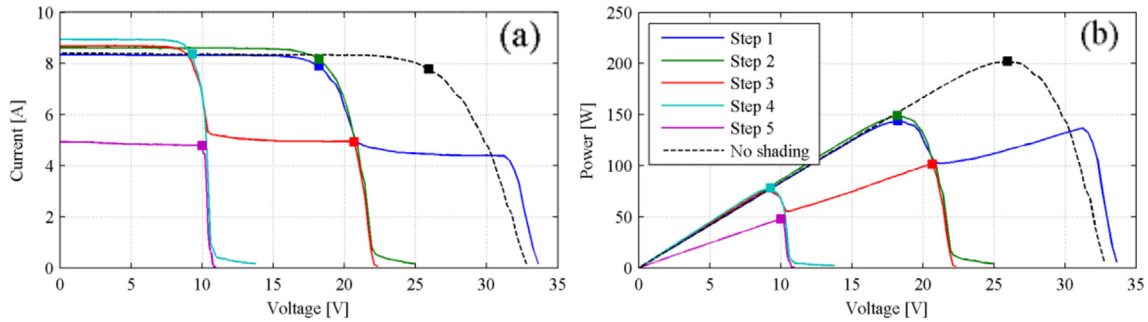

Fig. 11. Recorded characteristics of poly-crystalline modules, referred to 1000 W/m^2: (a) current–voltage, and (b) power–voltage. Diagonally shading process.

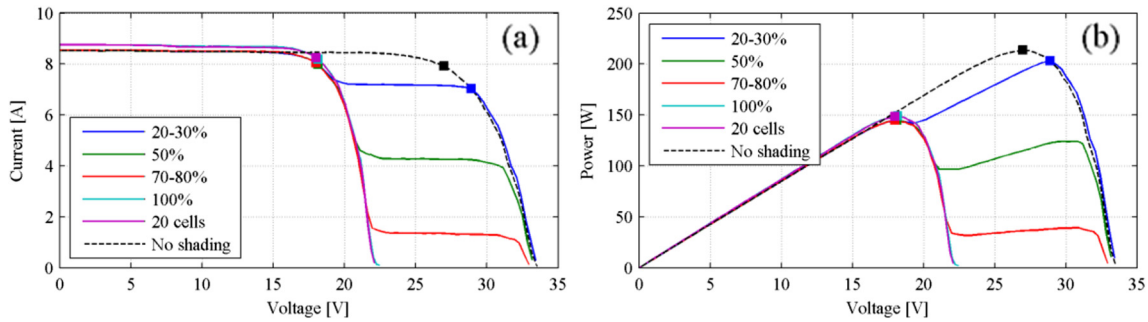

Fig. 12. Recorded characteristics of mono-crystalline modules, referred to 1000 W/m^2: (a) current–voltage, and (b) power–voltage. Vertically shading profile.

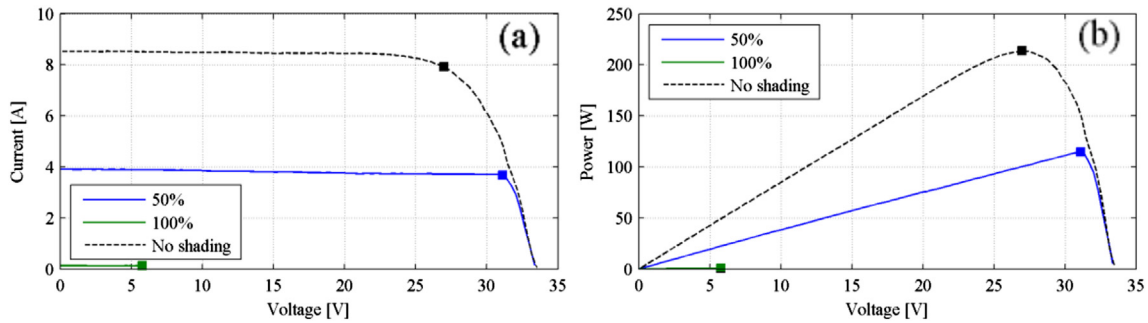

Fig. 13. Recorded characteristics of mono-crystalline modules, referred to 1000 W/m^2: (a) current–voltage, and (b) power–voltage. Horizontally shading profile.

Fig. 11, respectively Fig. 14, illustrates the current–voltage and power–voltage curves of a poly-crystalline, respectively mono-crystalline, PV module diagonally shaded from step 1 to step 5, and without shading. The points (V_{MPP}, I_{MPP}) and (V_{MPP}, P_{MPP}), for each shading condition, are illustrated.

3.3. Discussion

As illustrated in Figs. 5–8, the generated current is decreasing as the shading profile is varied between 0% and 100%. For a 100% shaded cell, the 20 series-connected cells of the subsection

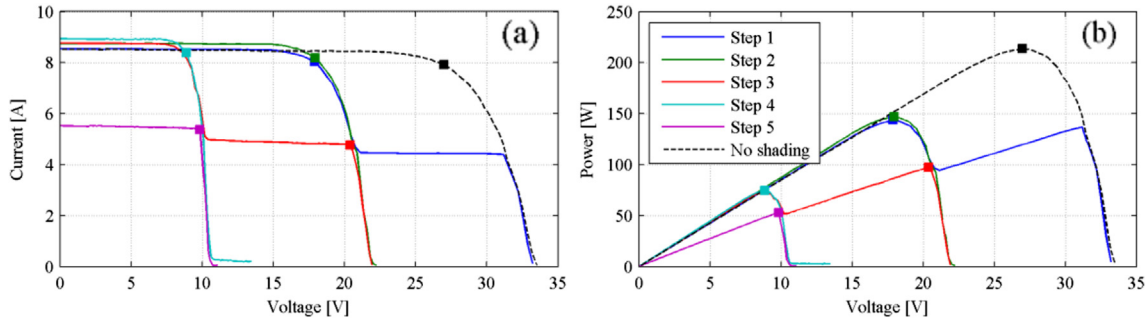

Fig. 14. Recorded characteristics of mono-crystalline modules, referred to 1000 W/m^2: (a) current–voltage, and (b) power–voltage. Diagonally shading profile.

Please cite this article in press as: Dolara A, et al., Experimental investigation of partial shading scenarios on PV (photovoltaic) modules, Energy (2013), http://dx.doi.org/10.1016/j.energy.2013.04.009

Table 3
Shading scenarios of a PV single-cell.

Mc	Shading scenario									
Pc	0%		25%		50%		75%		100%	
Right-to-left										
I_{MPP} [A]	7.79	7.93	6.45	6.98	7.82	7.97	7.79	7.94	8.01	8.17
V_{MPP} [V]	25.95	26.97	28.90	29.14	17.72	18.13	17.77	18.15	17.76	18.06
P_{MPP} [W]	202.1	213.9	186.4	203.4	138.6	144.4	138.4	144.1	142.3	147.6
$P_{MPP,x\%}/P_{MPP,0\%}\cdot 100$ [%]	100	100	92.2	95.1	68.6	67.5	68.5	67.4	70.4	69.0
Bottom-to-top										
I_{MPP} [A]	7.79	7.93	5.92	29.85	7.85	7.95	7.83	7.99	8.01	8.17
V_{MPP} [V]	25.95	26.97	29.31	5.91	17.76	18.15	17.67	18.07	17.76	18.06
P_{MPP} [W]	202.1	213.9	173.6	176.5	138.7	144.3	138.4	144.4	142.3	147.6
$P_{MPP,x\%}/P_{MPP,0\%}\cdot 100$ [%]	100	100	85.9	82.5	68.6	67.5	68.5	67.5	70.4	69.0

interested by shadowing are not generating and short-circuited by the by-pass diode, and thus only 2/3 of the module is producing. The results obtained for the poly-crystalline modules are very close to those obtained for the mono-crystalline ones. Small differences of voltage and current values at MPP are related to the different module's technology, to the tolerance in positioning the shading obstacle, and to the temperature reached by the different modules during performed test. For brevity, only the measurement results on poly-crystalline modules are recalled within the text. The measured values for both module technologies are reported in Tables 3 and 4.

The results, obtained during the performed experiments by shading a PV single-cell, are synthesized in Table 3. Without shading, the maximum power of the PV module is $P_{MPP,0\%} = 202.1$ W at $V_{MPP,0\%} = 25.95$ V. When shading occurs, a significant reduction of the output power is noted and two maximum points appear on the power–voltage curve. The analysis of the influence of cell type in reverse bias, amount of shading, and the number of shaded cells of a test module is conducted in Ref. [44].

The maximum power production decreases critically for the 50% shading scenario ($P_{MPP,50\%} = 138.6$ W for the right-to-left shading profile, respectively $P_{MPP,50\%} = 138.7$ W for the bottom-to-top

Table 4
Shading scenarios of a PV module.

Mc	Shading scenario									
Pc	0%		25%		50%		75%		100%	
Vertical profile										
I_{MPP} [A]	7.79	7.93	6.43	7.04	7.82	7.99	7.87	8.05	7.99	8.20
V_{MPP} [V]	25.95	26.97	28.95	28.91	17.95	18.14	17.70	17.99	18.41	18.16
P_{MPP} [W]	202.1	213.9	186.1	203.4	140.3	144.96	139.3	144.9	147.1	148.8
$P_{MPP,x\%}/P_{MPP,0\%}\cdot 100$ [%]	100	100	92.1	95.1	69.4	67.8	68.9	67.7	72.3	69.6
Horizontal profile										
I_{MPP} [A]	7.79	7.93			2.07	3.68			0.24	0.14
V_{MPP} [V]	25.95	26.97			29.95	31.11			19.28	5.77
P_{MPP} [W]	202.1	213.9			62.0	114.4			4.59	0.79
$P_{MPP,x\%}/P_{MPP,0\%}\cdot 100$ [%]	100	100			30.7	53.5			2.2	0.3

Mc	Diagonal profile									
Pc	Step 0		Step 1		Step 2		Step 3		Step 4		Step 5	
I_{MPP} [A]	7.79	7.93	7.90	8.04	8.18	8.19	4.92	4.77	8.37	8.39	4.78	5.37
V_{MPP} [V]	25.95	26.97	18.23	17.89	18.21	17.95	20.67	20.39	9.30	8.87	10.02	9.84
P_{MPP} [W]	202.1	213.9	144.0	143.9	148.9	147.0	101.7	97.3	78.0	74.5	47.9	52.9
$P_{MPP,x\%}/P_{MPP,0\%}\cdot 100$ [%]	100	100	71.3	67.3	73.7	68.7	50.3	45.5	38.6	34.8	23.7	24.7

Please cite this article in press as: Dolara A, et al., Experimental investigation of partial shading scenarios on PV (photovoltaic) modules, Energy (2013), http://dx.doi.org/10.1016/j.energy.2013.04.009

shading profile). Above this value, the MPP points are located very far from the normal MPP region ($P_{MPP,100\%}$ = 142.3 W at $V_{MPP,100\%}$ = 17.76 V) and depends only on the two unshaded sections of the PV module.

As illustrated in Figs. 5–8 and reported also in Table 3, the module's power generation by shading a single-cell is not depending in a critical manner on the shading profile (right-to-left and bottom-to-top), as well as on the poly-crystalline or mono-crystalline typology.

The results, obtained during the performed experiments by shading a PV module, are synthesized in Table 4. As illustrated in Figs. 9–14, the generated current is decreasing as the shading profile is varied between 0% and 100%.

The vertical shading of the module determines similar results as the ones obtained by shading a single-cell. Because the cells have a series connection, shading one cell or shading a column of 10 series-connected cells determine the same result ($P_{MPP,50\%}$ = 140.3 W at $V_{MPP,50\%}$ = 17.95 V). Similarly, shading a line of cells or shading two lines of cells composing a module's subsection lead to the same result.

The horizontal shading of the module influences all the three module's subsections. In this case, the generated current critically decreases until becomes zero when an entire horizontal line of cells is shaded ($P_{MPP,100\%}$ = 4.59 W at $I_{MPP,100\%}$ = 0.24 A and $V_{MPP,100\%}$ = 19.28 V).

As illustrated in Figs. 11 and 14, the diagonal shading determines a decrease of the generated current as the shading profile is varied between step 1 and step 5. As illustrated in Figs. 11 and 14, the diagonal shading determines a decrease of the generated current as the shading profile is varied between step 1 and step 5. For the step 1 of the diagonal shading profile (one single-cell is 50% shaded), the module generates the electrical current $I_{MPP,\ step\ 1}$ = 7.90 A as much as when a PV single-cell is 50% shaded. As illustrated in Figs. 11 and 14, for the step 2 of the diagonal shading profile (one cell is completely shaded and two cells are 50% shaded), the electrical current generated by the shaded subsection of the module becomes zero. Above step 3, the MPP points are located very far from the normal MPP region ($P_{MPP,\ step\ 4}$ = 78.0 W at $V_{MPP,\ step\ 4}$ = 9.3 V). This behavior is observed also for the third module's subsection, when step 5 is considered.

As illustrated in Figs. 9–14 and reported also in Table 4, the module's power production is not depending in a critical manner on the poly-crystalline or mono-crystalline typology.

4. Conclusions

In this paper, the effects of partial shading on poly-crystalline and mono-crystalline photovoltaic modules performance are analyzed. The performed experimental tests provide an investigation of shadow effects on the main electrical characteristics of the PV modules. In particular, a large difference in the performances of the two PV typologies is not observed.

The bypass diodes of the PV modules are highly important. These diodes allow dividing in several sections each module, limiting the production's decrease caused by the shading conditions. The results show that the generated current is decreasing as the shading profile is varied between 0% and 100%. The experimental results report that, by shading 50% of a PV single-cell, the power production of the PV module is reducing by more than 30%. The vertically, horizontally, and diagonally shading profiles applied to PV module determine similar results as the ones obtained by shading a single-cell.

The conducted analysis can be used to derive mathematical models for evaluating the power losses caused by shading conditions influencing PV modules operation.

References

[1] Mathiesen BV, Lund H, Karlsson K. 100% renewable energy systems, climate mitigation and economic growth. Applied Energy 2011;88(2):488–501.
[2] Lund H, Mathiesen BV. Energy system analysis of 100% renewable energy systems – the case of Denmark in years 2030 and 2050. Energy 2009;34(5):524–31.
[3] Carcangiu G, Dainese C, Faranda R, Leva S, Sardo M. New network topologies for large scale photovoltaic systems. In: Proceedings of the IEEE power tech conference 2009. p. 1–7. Bucharest, RO.
[4] Dolara A, Grimaccia F, Leva S, Mussetta M, Faranda R, Gualdoni M. Performance analysis of a single-axis tracking PV system. IEEE Journal of Photovoltaics 2012;2:524–31.
[5] Kadri R, Andrei H, Gaubert JP, Ivanovici T, Champenois G, Andrei P. Modeling of the photovoltaic cell circuit parameters for optimum connection model and real-time emulator with partial shadow conditions. Energy 2012;42(1):57–67.
[6] Rehman S, El-Amin I. Performance evaluation of an off-grid photovoltaic system in Saudi Arabia. Energy 2012;46:451–8.
[7] Wang JC, Shieh JC, Su YL, Kuo KC, Chang YW, Liang YT, et al. A novel method for the determination of dynamic resistance for photovoltaic modules. Energy 2011;36:5968–74.
[8] Jiang JA, Wang JC, Kuo KC, Su YL, Shieh JC, Chou JJ. Analysis of the junction temperature and thermal characteristics of photovoltaic modules under various operation conditions. Energy 2012;44:292–301.
[9] Woyte V, Nijs J, Belmans R. Partial shadowing of photovoltaic arrays with different system configurations: literature survey and field results. Solar Energy 2003;74(3):217–33.
[10] Paraskevadaki EV, Papathanassiou SA. Evaluation of MPP voltage and power of mc-Si PV modules in partial shading conditions. IEEE Transactions on Energy Conversion 2011;26(3):923–32.
[11] Lam KH, Lai TM, Lo WC, To WM. The application of dynamic modelling techniques to the grid-connected PV (photovoltaic) systems. Energy 2012;46:264–74.
[12] Bishop JW. Computer simulation of the effects of electrical mismatches in photovoltaic cell interconnection circuit. Solar Cells 1988;25:73–89.
[13] Quaschning V, Hanitsch R. Numerical simulation of current-voltage characteristics of photovoltaic systems with shaded cells. Solar Energy 1996;56(6):513–20.
[14] Ramaprabha R, Mathur BL. Impact of partial shading on solar PV module containing series connected cells. International Journal of Recent Trends in Engineering 2009;2(7):56–60.
[15] Mäki A, Valkealahti S. Power losses in long string and parallel-connected short strings of series-connected silicon-based photovoltaic modules due to partial shading conditions. IEEE Transactions on Energy Conversion 2012;27(1):173–83.
[16] Al-Rawi NA, Al-Kaisi MM, Asfer D. Reliability of photovoltaic modules II. Interconnections and bypass diodes effects. Solar Energy Materials and Solar Cells 1994;31(4):469–80.
[17] Alonso-Garcia MC, Ruiz JM. Analysis and modelling the reverse characteristic of photovoltaic cells. Solar Energy Materials and Solar Cells 2006;90(7):1105–20.
[18] Silvestre S, Boronat A, Chouder A. Study of bypass diodes configuration on PV modules. Applied Energy 2009;86(9):1632–40.
[19] Kawamura H, Naka K, Yonekura N, Yamanaka S, Kawamura H, Ohno H, et al. Simulation of I–V characteristics of a PV module with shaded PV cells. Solar Energy Materials and Solar Cells 2003;75(3):613–21.
[20] Alonso-Garcia MC, Ruiz JM, Herrmann W. Computer simulation of shading effects in photovoltaic arrays. Renewable Energy 2006;31(12):1986–93.
[21] Wang YJ, Hsu PC. Analytical modelling of partial shading and different orientation of photovoltaic modules. IET Renewable Power Generation 2010;4(3):272–82.
[22] Liu G, Nguang SK, Partridge A. A general modeling method for I–V characteristics of geometrically and electrically configured photovoltaic arrays. Energy Conversion and Management 2011;52(12):3439–45.
[23] Meyer EL, Van Dyk EE. The effect of reduced shunt resistance and shading on photovoltaic module performance. In: Proceedings of the 31st IEEE photovoltaic specialists conference 2005. p. 1331–4. Orlando, FL.
[24] Van Der Borg NJCM, Jansen MJ. Energy loss due to shading in a BIPV application. In: Proceedings of the 3rd world conference on photovoltaic energy conversion 2003. p. 2220–2. Osaka, Japan.
[25] Patel H, Agarwal V. MATLAB-based modeling to study the effects of partial shading on PV array characteristics. IEEE Transactions on Energy Conversion 2008;23(1):302–10.
[26] Gow JA, Manning CD. Development of a photovoltaic array model for use in power-electronics simulation studies. IEE Proceedings-Electric Power Applications 1999;146(2):193–200.
[27] Castaner L, Silvestre S. Modelling photovoltaic systems using PSpice. New York: John Wiley & Sons; 2003.
[28] Veerachary M. PSIM circuit-oriented simulator model for the nonlinear photovoltaic sources. IEEE Transactions on Aerospace and Electronic Systems 2006;42(2):735–40.
[29] Wang YJH. An investigation on partial shading of PV modules with different connection configurations of PV cells. Energy 2011;36(5):3069–78.

Please cite this article in press as: Dolara A, et al., Experimental investigation of partial shading scenarios on PV (photovoltaic) modules, Energy (2013), http://dx.doi.org/10.1016/j.energy.2013.04.009

[30] Yazdani A, Di Fazio AR, Ghoddami H, Russo M, Kazerani M, Jatskevich J, et al. Modeling guidelines and a benchmark for power system simulation studies of three-phase single-stage photovoltaic systems. IEEE Transaction on Power Delivery 2011;26(2):1247–64.
[31] Esram T, Chapman PL. Comparison of photovoltaic array maximum power point tracking techniques. IEEE Transactions on Energy Conversion 2007;22(2):439–49.
[32] Garcia M, Maruri JM, Marroyo L, Lorenzo E, Perez M. Partial shadowing, MPPT performance and inverter configurations: observations at tracking PV plants. Progress in Photovoltaics: Research and Applications 2008;16: 529–36.
[33] Picault D, Raison B, Bacha S, de la Casa J, Aguilera J. Forecasting photovoltaic array power production subject to mismatch losses. Solar Energy 2010;84(7): 1301–9.
[34] Gao L, Dougal R, Liu S, Iotova AP. Parallel-connected solar PV system to address partial and rapidly fluctuating shadow conditions. IEEE Transactions on Industrial Electronics 2009;56(5):1548–56.
[35] Ramaprabha R, Mathur BL. A comprehensive review and analysis of solar photovoltaic array configurations under partial shaded conditions. International Journal of Photo Energy 2012;12(February):1–16.
[36] Brenna M, Dolara A, Foiadelli F, Lazaroiu GC, Leva S. Transient analysis of large scale PV systems with floating DC section. Energies 2012;5:3736–52.
[37] Súri M, Huld TA, Dunlop ED. PVGIS: a web-based solar radiation database for the calculation of PV potential in Europe. International Journal of Sustainable Energy 2005;24:55–67.
[38] IEC 60904-1. Photovoltaic devices. Part 1: measurements of photovoltaic current–voltage characteristics. 1st ed. Geneve: International Electrotechnical Commission IEC-60904-1; 2006.
[39] IEC 60891. Photovoltaic devices. Procedures for temperature and irradiance corrections to measured I–V characteristics. 1st ed. Geneve: International Electrotechnical Commission IEC 60891; 2010.
[40] IEC 62446. Grid connected photovoltaic systems-minimum requirements for system documentation, commissioning test and inspection. 1st ed. Geneve: International Electrotechnical Commission IEC 62446; 2009.
[41] Muñoz JV, Nofuentes G, Aguilera J, Fuentes M, Vidal PG. Procedure to carry out quality checks in photovoltaic grid-connected systems: six cases of study. Applied Energy 2011;88:2863–70.
[42] LSI. Global radiation sensors. Milan. Available from: http://www.lsi-lastem.it/prodotti.php?prod_cat_id=165; 2012 [accessed 01.02.13].
[43] LSI. Global radiation sensors. Milan. Available from: http://www.lsi-lastem.it/prodotti.php?prod_cat_id=162; 2012 [accessed 01.02.13].
[44] Alonso-García M, Ruiz J, Chenlo F. Experimental study of mismatch and shading effects in the I–V characteristic of a photovoltaic module. Solar Energy Materials and Solar Cells 2006;90:329–40.

Please cite this article in press as: Dolara A, et al., Experimental investigation of partial shading scenarios on PV (photovoltaic) modules, Energy (2013), http://dx.doi.org/10.1016/j.energy.2013.04.009